

Supplementary Data

Supplementary Table 1 – Demographic and clinicopathological features of cases¹

		N	%
ER Status	Negative	102	41%
	Positive	145	59%
TNM Stage	<= II	184	71%
	>= III	44	29%
Grade	1 & 2	108	50%
	3	107	50%
Race ²	AA	143	58%
	EA	105	42%
p53 mutation	Negative	200	81%
	Positive	48	19%
Chemotherapy ³	No	99	43%
	Yes	132	57%
NOS2	Negative	43	17%
	Weak	32	13%
	Moderate	72	29%
	High	101	41%
Survival	Alive	163	66%
	Death from breast cancer	74	30%
	Death from other causes	11	4%
Breast Cancer Subtypes			
ER+ (“Luminal A”)		83	33%
ER+/HER2+ (“Luminal B”) ⁴		61	25%
Basal-like (IHC-based)		41	16%
ER-/HER2+		32	13%
Triple-negative (ER-/PR-/HER2-) ⁵		56	23%
		mean ± SD	
Age at Diagnosis (n = 248)		55.0 ± 13.9	
Body mass index (n = 236)		29.0 ± 8.1	
CD31 (n = 208) ⁶		49.1 ± 43.9	
CD68 (n = 247) ⁷		97.3 ± 56.9	

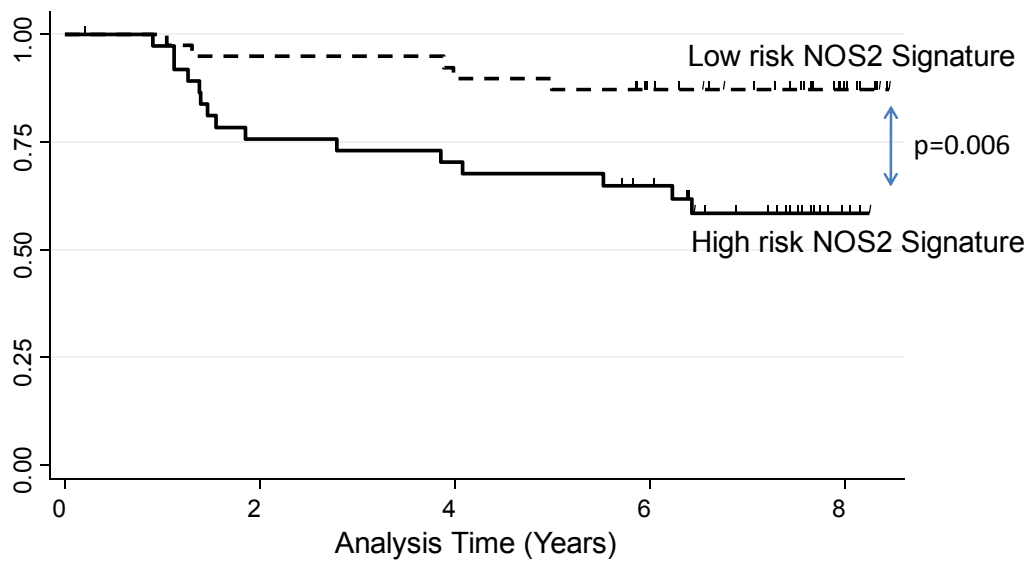
¹Cases with missing information are not included. SD = standard deviation. Race/ethnicity is determined by self-identification. ²AA=African-American, EA=European-American. ³Includes neoadjuvant therapy. ⁴Few luminal B tumors are HER2-negative. ⁵PR status was not available for all tumors in the study. ⁶Number of CD31-positive microvessels per 200x field in the most vascular regions of the tumor as average of 3 representative fields. ⁷Number of CD68-positive monocytes/macrophages per 250x field as average of 3 representative fields.

Supplementary Table 2 – Publications linking NOS2 gene signature to basal-like breast cancer

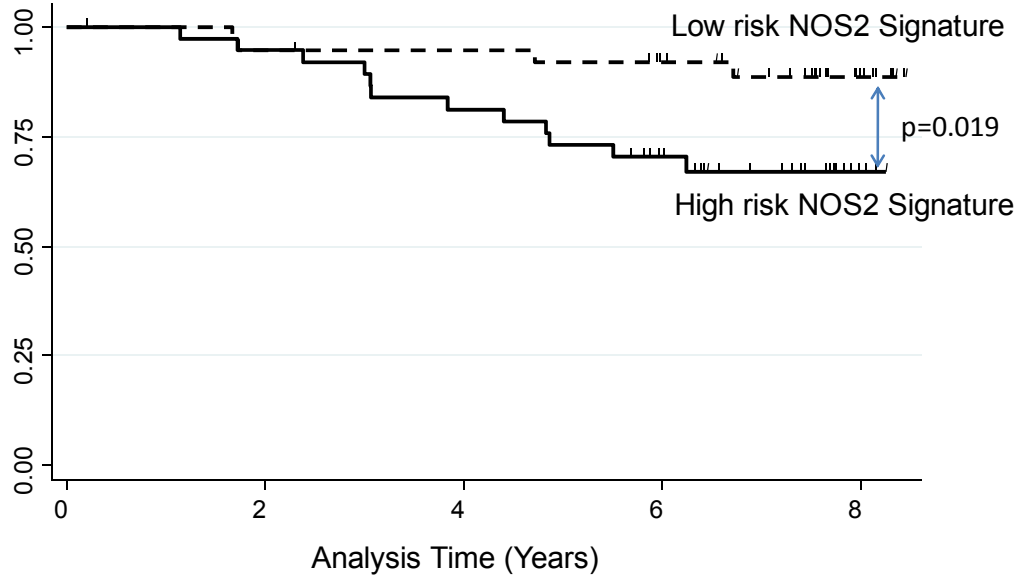
GenBankID	Gene Symbol	Publications Linking to Basal-like breast cancer
AL569511	<i>KRT6A/B/C/E</i>	Livasy, Rakha , Charafe-Jauffret,
J00269	<i>KRT6A/C/E</i>	Livasy, Rakha, Charafe-Jauffret
NM_021804	<i>ACE2</i>	
L42612	<i>KRT6B</i>	Livasy, Charafe-Jauffret
AI831452	<i>KRT6B</i>	Livasy, Charafe-Jauffret
NM_025087	<i>FLJ21511</i>	
NM_000422	<i>KRT17</i>	Dabbs, Charafe-Jauffret, Sorlie
Z19574	<i>KRT17</i>	Dabbs, Charafe-Jauffret, Sorlie
NM_000584	<i>IL8</i>	
NM_003064	<i>SLPI</i>	Charafe-Jauffret, Sorlie
NM_018004	<i>TMEM45A</i>	
NM_002964	<i>S100A8</i>	Charafe-Jauffret, Sorlie
L25541	<i>LAMB3</i>	Charafe-Jauffret
NM_001793	<i>CDH3</i>	Arnes, Matos, Paredas, Potemski, Charafe-Jauffre
AB018009	<i>SLC7A5</i>	
NM_018455	<i>C16orf60</i>	
X57348	<i>SFN</i>	Leibl, Charafe-Jauffret
NM_001630	<i>ANXA8</i>	Stein, Charafe-Jauffret
NM_005629	<i>SLC6A8</i>	
NM_012101	<i>TRIM29</i>	Charafe-Jauffret
NM_002061	<i>GCLM</i>	
AF132818	<i>KLF5</i>	Charafe-Jauffret, Sorlie,
NM_022121	<i>PERP</i>	Charafe-Jauffret, Sorlie
NM_003878	<i>GGH</i>	
NM_007196	<i>KLK8</i>	Sorlie
NM_016593	<i>CYP39A1</i>	Sorlie
NM_003662	<i>PIR</i>	
NM_001047	<i>SRD5A1</i>	Sorlie
X57348	<i>SFN</i>	Leibl, Charafe-Jauffret
NM_005342	<i>HMGB3</i>	
NM_006623	<i>PHGDH</i>	Sorlie
AV712602	<i>PTPLB</i>	Sorlie
X16447	<i>CD59</i>	Charafe-Jauffret
NM_003392	<i>WNT5A</i>	
NM_000611	<i>CD59</i>	Charafe-Jauffret
BE964473	<i>RPE</i>	
NM_000050	<i>ASS</i>	
NM_002633	<i>PGM1</i>	
D84454	<i>SLC35A2</i>	
BF116254	<i>TPI1</i>	
NM_005333	<i>HCCS</i>	Sorlie
NM_001428	<i>ENO1</i>	
NM_000610	<i>CD44</i>	Charafe-Jauffret
BF939365	<i>CALU</i>	
NM_014637	<i>MTFR1</i>	
NM_000365	<i>TPI1</i>	
AF289489	<i>ASPH</i>	
BC003375	<i>MRPL3</i>	
AI186712	<i>PPP1CB</i>	

A

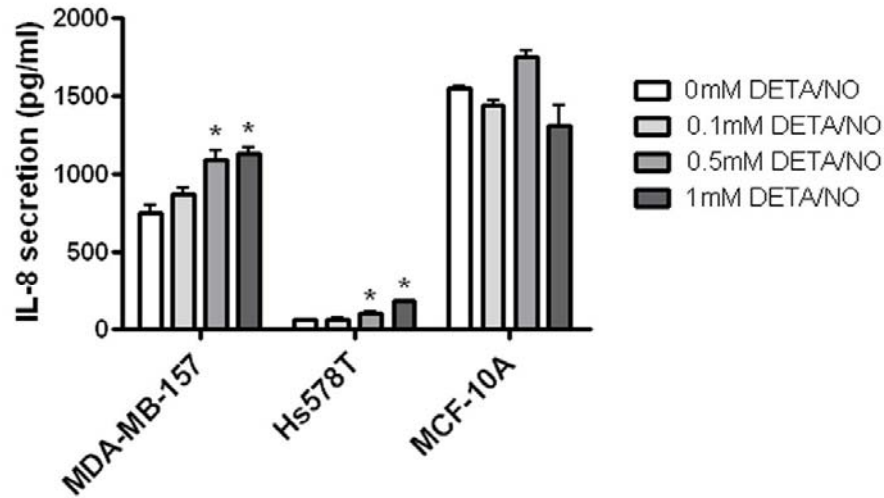
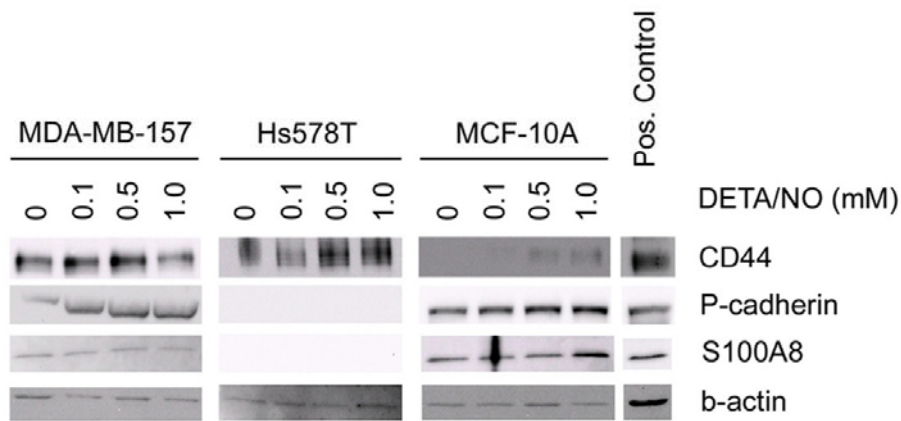
% Relapse – ER negative Karolinska

**B**

% Survival – ER negative Karolinska

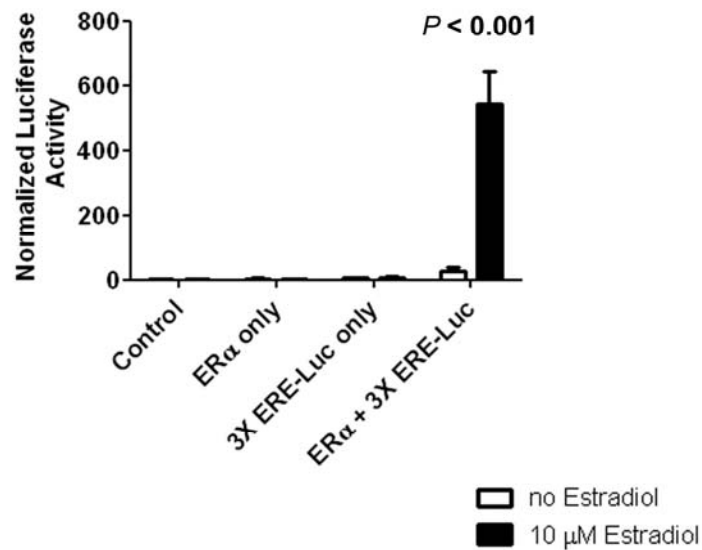
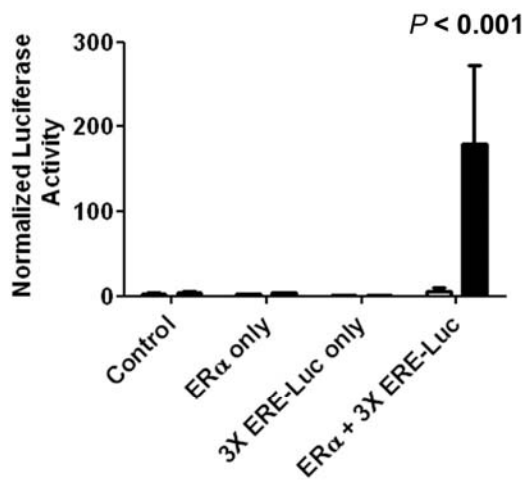


Supplementary Figure 1 – NOS2 gene signature predicts survival in ER-negative breast cancer cases from the Karolinska data set. (A) Relapse-free survival. (B) Overall survival. Patients with the NOS2 gene signature (high risk NOS2 signature) have significantly poorer survival than patients without it (low risk NOS2 signature).

A**B**

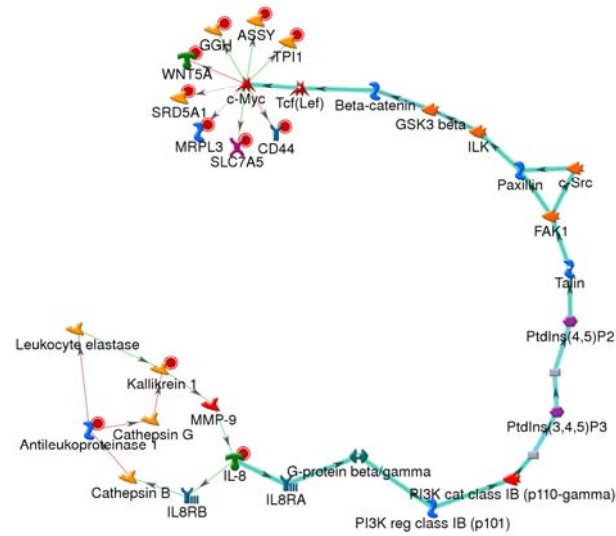
Supplementary Figure 2 – Induction of IL-8, S100A8, CD44, and P-cadherin in ER-negative epithelial breast cell lines after exposure to the NO donor, DETA/NO.

(A) DETA/NO induced IL-8 secretion in the two ER-negative breast cancer cell lines, MDA-MB-157 and Hs578T, over a 48 hr exposure, but not in the ER-negative, non-tumorigenic MCF-10A cells. Shown are mean \pm SD. * $P < 0.05$ student's t-test. (B) Induction of CD44, P-cadherin and S100A8 in the ER-negative cell lines MDA-MB-157, Hs578T, and MCF10A cells, over a 48hr exposure. Hs578T cells did not express P-cadherin and S100A8 at a detectable level.

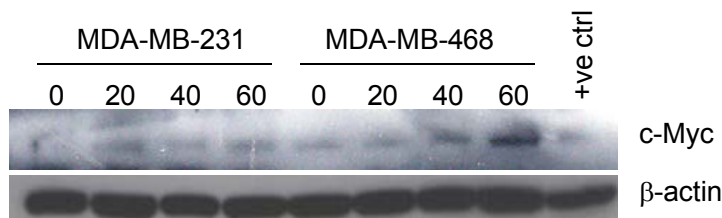
A**B**

Supplementary Figure 3 – ER α transcriptional activity in ER-negative breast cancer cells after transfection with an estrogen receptor α expression plasmid. (A) MDA-MB-231 and (B) MDA-MB-468 cells were transfected with an expression plasmid for the estrogen receptor α (ER α) and the transcriptional activity of the expressed receptor in these cells was determined with a luciferase reporter construct containing 3 estrogen response elements (3X ERE-Luc). The reporter was activated in the two cell lines by the ER α transgene, which was dependent on β -estradiol in the culture medium. Shown is mean \pm SD for the luciferase activity.

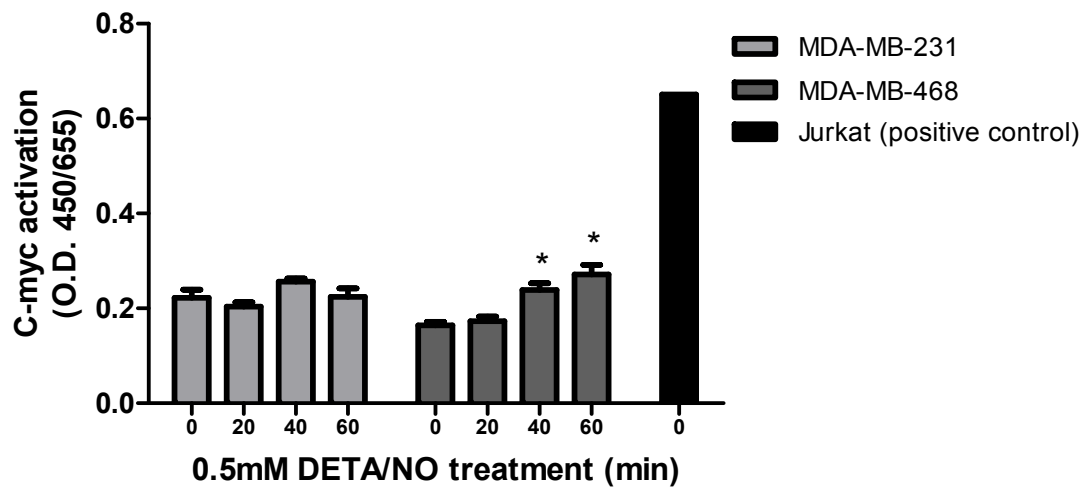
(A)



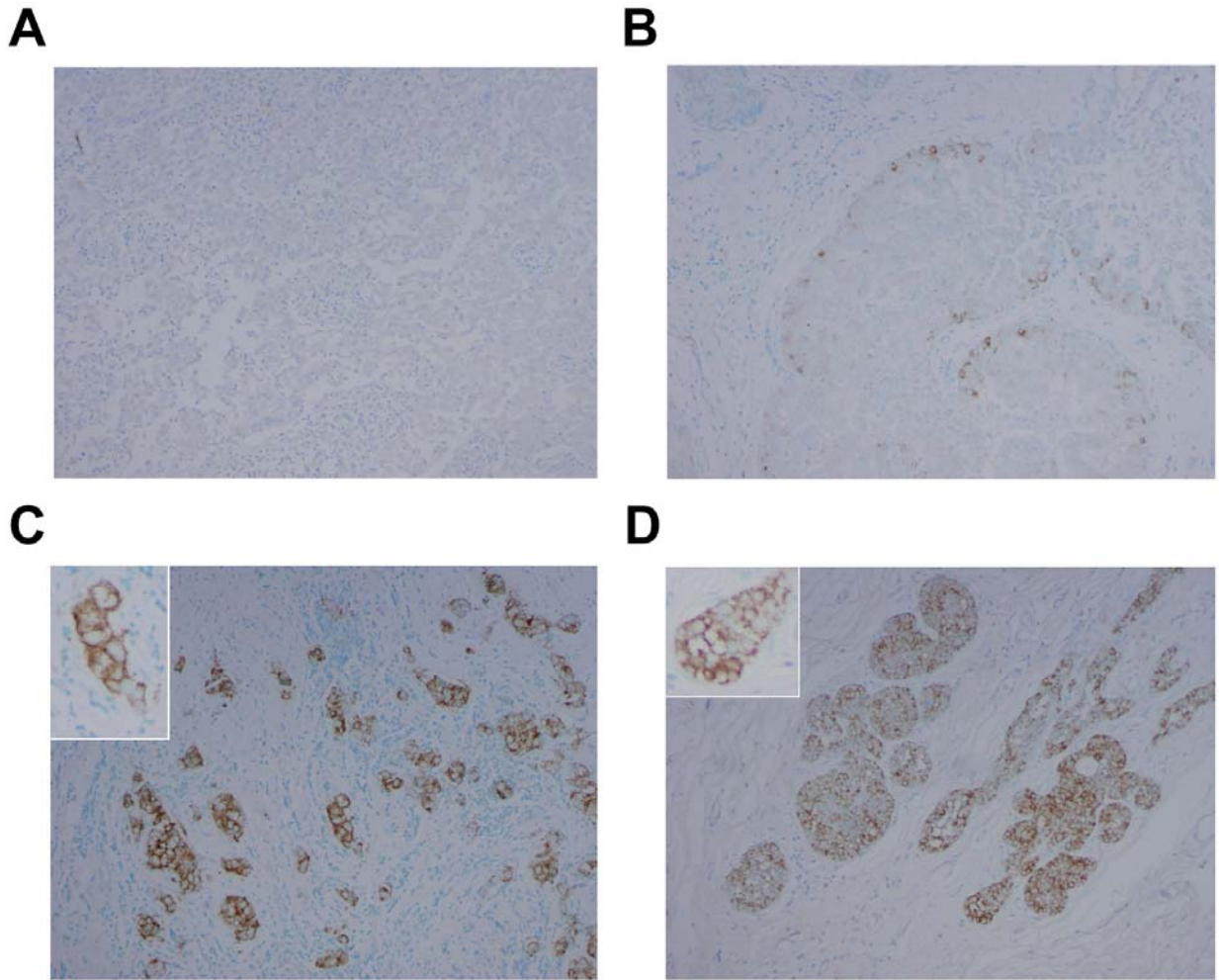
(B)



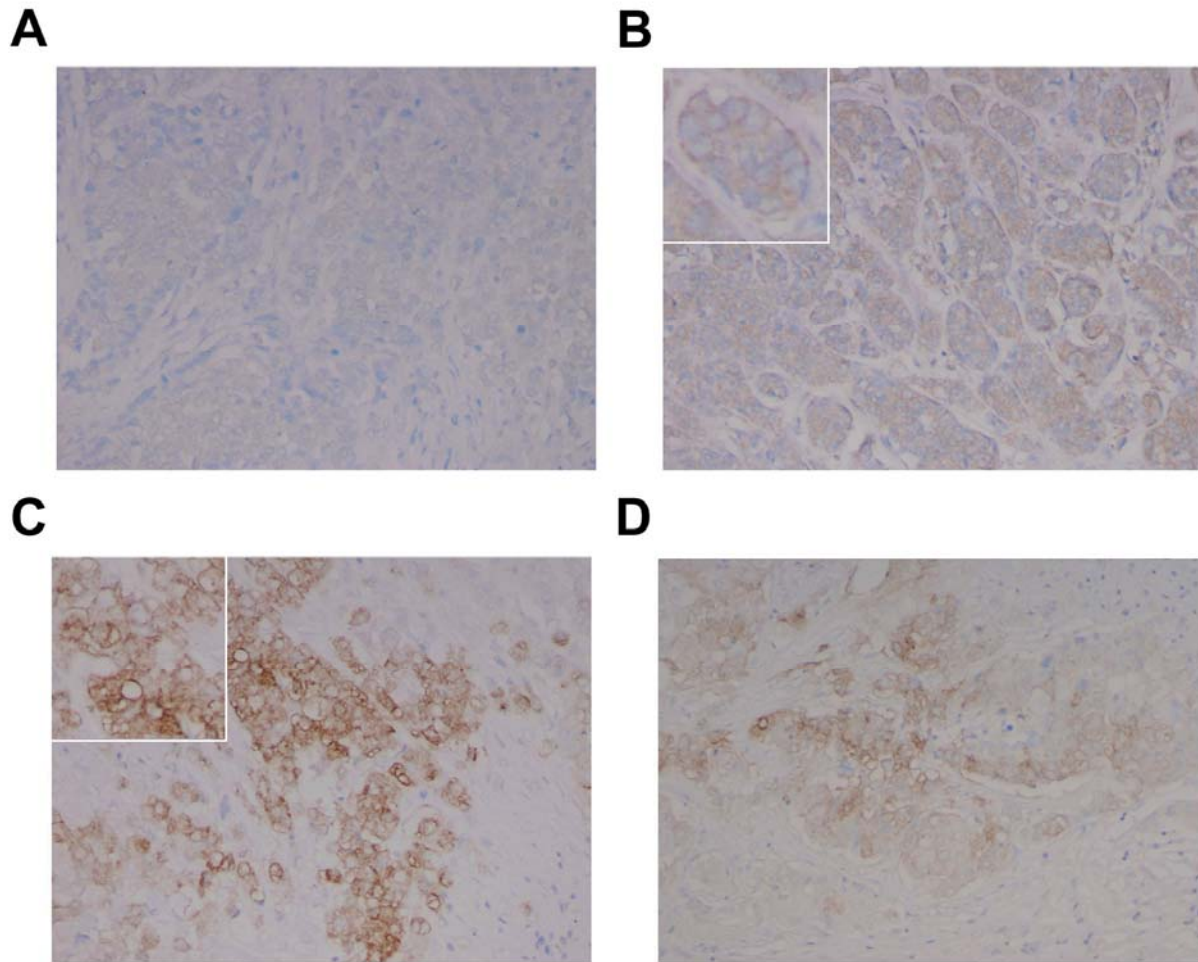
(C)



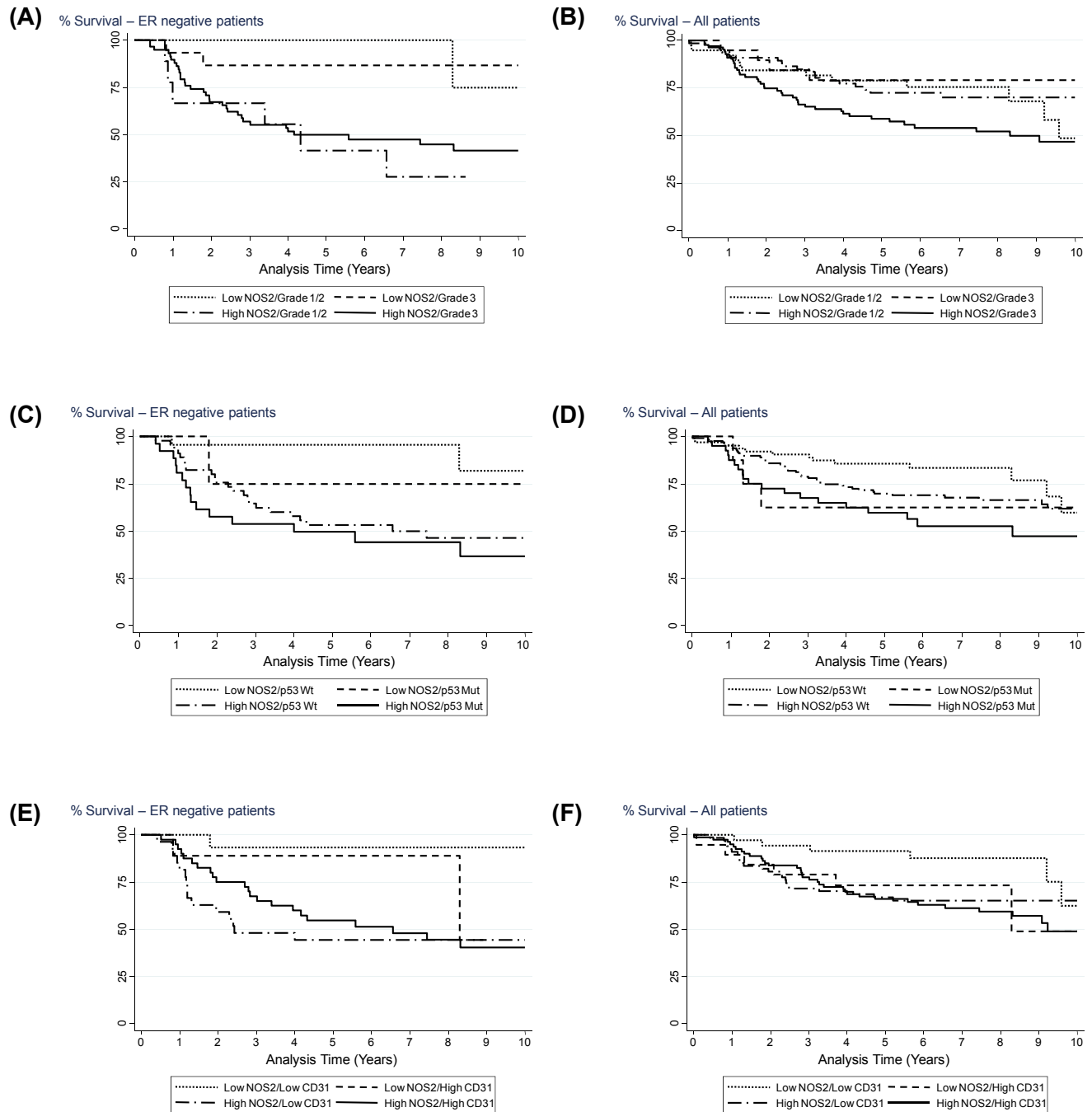
Supplementary Figure 4 – Induction of c-Myc by the NO donor, DETA/NO. (A) Metacore pathway analysis suggesting putative linkage of the NOS2 signature to c-Myc. (B) 0.5 mM DETA/NO increased c-Myc protein expression in MDA-MB-468 cells within 60 minutes of exposure. This effect was not observed in MDA-MB-231 cells. Positive control (ve ctrl) is a Jurkat cell extract. (C) 0.5 mM DETA/NO induced c-Myc activation in MDA-MB-468 cells within 60 minutes of exposure. This effect was not observed in MDA-MB-231 cells. Mean \pm SD.



Supplementary Figure 5 – EGFR expression in human breast tumors. IHC analysis of invasive breast carcinomas for expression of epidermal growth factor receptor (EGFR) (A-D). EGFR was mainly detected in the cell membrane of tumor cells with some cells also showing a cytoplasmic staining of the protein. EGFR expression was not detectable in a subset of tumors (A). The pattern of EGFR expression ranged from few tumor cells being EGFR positive (B) to all tumor cells being positive for EGFR (C,D). Magnification: 100X for A,B,D; 200X for C. Counterstain: Methyl Green.



Supplementary Figure 6 – Phosphorylation of EGFR at tyrosine 1173 in human breast tumors. Analysis of invasive breast tumors for presence and distribution of pEGFR tyr1173 (A-D). Tumor without detectable phosphorylation of EGFR at tyrosine 1173 (A). When noticeable, phosphorylated EGFR was predominately membrane-bound but also cytoplasmic (B-D), and was either equally evident in all tumor cells (B) or was heterogeneous in intensity among the tumor cells (C,D). Magnification: 100X. Counterstain: Methyl Green.



Supplementary Figure 7 – Influence of tumor grade, p53 mutation status, and microvessel density on NOS2-related patient survival. Kaplan-Meier cumulative breast cancer-specific survival curves of (A) ER-negative breast cancer patients by NOS2 and tumor grade (n = 89). Log-rank test: $P < 0.015$. (B) All breast cancer patients (n = 206). $P < 0.039$; (C) ER-negative breast cancer patients by NOS2 and p53 mutation status (n = 98). $P < 0.004$. (D) All breast cancer patients (n = 238). $P < 0.042$; (E) ER-negative breast cancer patients by NOS2 and microvessel density (= CD31 count) (n = 91). $P < 0.008$. (F) All breast cancer patients (n = 201). $P < 0.129$. A cutoff at the median was used to define a low/high tumor CD31 count.